Perturbative determination of $O(a)$ boundary improvement coefficients for the Schrödinger functional coupling at 1 loop with improved gauge actions

Shinji Takeda, Sinya Aoki, and Kiyotomo Ide
Institute of Physics, University of Tsukuba, Ibaraki 305-8571, Japan
(Received 22 April 2003; published 10 July 2003)

We determine $O(a)$ boundary improvement coefficients up to the 1-loop level for the Schrödinger functional coupling with improved gauge actions including plaquette and rectangle loops. These coefficients are required to implement 1-loop $O(a)$ improvement in full QCD simulations for the coupling with the improved gauge actions. To this order, lattice artifacts of the step scaling function for each improved gauge action are also investigated. In addition, passing through the Schrödinger functional scheme, we estimate more accurately the ratio of the Λ parameters between the improved gauge actions and the plaquette action.

DOI: 10.1103/PhysRevD.68.014505 PACS number(s): 11.15.Ha

I. INTRODUCTION

The modified minimal subtraction ($\overline{\mathrm{MS}}$) scheme has now become the standard renormalization scheme for the definition of the strong coupling constant. The measured coupling constant α_s in some experiments at relatively high energy is converted to $\alpha_{\overline{\mathrm{MS}}}$ at some representative scale by perturbation theory. The current world average of such estimates gives $\alpha_{\overline{\mathrm{MS}}}(m_Z=91.19\ \mathrm{GeV})\approx 0.11$. Lattice QCD calculations, on the other hand, have the potential ability to determine the strong coupling constant from experimental input at a low (hadronic) energy scale. In order to compare the coupling constant obtained at low energy by lattice calculations with $\alpha_{\overline{\mathrm{MS}}}$ obtained at high energy, the Schrödinger functional scheme has been proposed by the ALPHA Collaboration [1], and the scheme has been shown to be successful. At present, the results on the running coupling constant of two massless flavor QCD have been reported [2,3].

In the real world there are three light quarks. QCD simulations including three dynamical quark effects are thus required to understand the low energy QCD dynamics. Our ultimate goal is to estimate $\alpha_{\overline{\mathrm{MS}}}$ from $N_f=3$ QCD simulations. Recently, the CP-PACS and JLQCD Collaborations have started an $N_f=3$ QCD simulation employing an exact fermion algorithm developed for an odd number of quark flavors [4–6]. In particular, noteworthy results were reported in [5]: There exist strong lattice artifacts associated with the phase transition in the $N_f=3$ QCD simulation with a combination of the plaquette gauge action and $O(a)$ improved Wilson quark action, while such lattice artifacts are absent for the renormalization group (RG) improved gauge action. Hence, the collaborations have decided to adopt the combination of the RG improved gauge action and $O(a)$ improved Wilson quark action for the $N_f=3$ QCD simulations to obtain $\alpha_{\overline{\mathrm{MS}}}$.

As a first step of our program, we study the Schrödinger functional coupling with improved gauge actions in perturbation theory. In particular, we perturbatively calculate the $O(a)$ boundary improvement coefficients at the 1-loop level with improved gauge actions for the pure SU(3) gauge theory. Combining these with the 1-loop results for the fermionic sector [7], we determine the $O(a)$ boundary improvement coefficients at 1-loop, which can be used for dynamical quark simulations in the future.

The rest of this paper is organized as follows. In Sec. II, after a brief reminder of the Schrödinger functional scheme and its extension to improved gauge actions, we specify the action used for later calculations and discuss the $O(a)$ boundary counterterm. In Sec. III the Schrödinger functional coupling constant is defined and formulas for determination of the $O(a)$ boundary improvement coefficients are given. The 1-loop computation is outlined in Sec. IV, and the results of the $O(a)$ boundary improvement coefficients are summarized in Sec. V. Our conclusion is given in the last section, together with a discussion of a lattice artifact of the step scaling function.

II. PRELIMINARIES

A. Schrödinger functional

It has been shown by the ALPHA Collaboration that the Schrödinger functional (SF) scheme is a powerful tool to probe the energy evolutions of some physical quantities and to compute improvement coefficients as well as renormalization constants. In the SF scheme, the theory is defined on a finite box of size $L^3\times T$ with periodic boundary conditions in the spatial directions and Dirichlet boundary conditions in the time direction. In the pure SU(3) gauge theory with Wilson plaquette action $S[U]$, the partition function in the SF scheme (in the case that $T=L$) is given by

$$\mathcal{Z}=\int D[U]e^{-S[U]}, \tag{2.1}$$

where the link variables $U(\mu,x)$ for the gauge fields satisfy the boundary conditions

$$U(x,k)|_{x_0=0}=\exp\{aC\},\quad U(x,k)|_{x_0=L}=\exp\{aC'\}. \tag{2.2}$$

Here a is the lattice spacing, and C,C' are diagonal traceless matrices, which depend on the background field parameters η and ν [8]. It has been shown [1] that the minimum of $S[U]$ is given by the lattice background field $U(x,\mu)=V(x,\mu)$, where

$$V(x,0)=1, \quad V(x,k)=V(x_0), \tag{2.3}$$

with

$$V(x_0)=\exp\{ab(x_0)\}, \tag{2.4}$$

$$b(x_0)=\frac{1}{L}[(L-x_0)C+x_0C']. \tag{2.5}$$

This background field represents a constant electric field.

An extension of the SF scheme to improved gauge actions was first considered by Klassen [9]. The transfer matrix construction [10] was adopted in the discussion. In this formulation, each boundary consists of two time slices, to achieved the tree-level $O(a^2)$ improvement.

In this paper, however, we adopt the formulation proposed by Aoki, Frezzotti, and Weisz [11], where each boundary consists of only one time slice and the tree-level $O(a)$ improvement is achieved. The dynamical variables to be integrated over are independent of the form of the action, whether plaquette or improved, and are given by the spatial link variables $U(k,x)$ with $x_0=a,\ldots,L-a$ and temporal link variables $U(0,x)$ with $x_0=0,\ldots,L-a$ on a cylinder with volume $L^3\times L$. This formulation is implemented more easily in numerical simulations.

The background field in Eq. (2.3) gives the local minimum of the theory in both cases [9] and [11]. It has not been theoretically proved, however, that Eq. (2.3) is the absolute minimum for the improved gauge actions. This has been checked only numerically [9].

B. Gauge action

Our improved action includes plaquette and rectangle loops and is given by

$$S_{\rm imp}[U]=\frac{1}{g_0^2}\sum_{\mathcal{C}\in\mathcal{S}_0} W_0(\mathcal{C},g_0^2)2\mathcal{L}(C) + \frac{1}{g_0^2}\sum_{\mathcal{C}\in\mathcal{S}_1} W_1(\mathcal{C},g_0^2)2\mathcal{L}(C), \tag{2.6}$$

with

$$\mathcal{L}(C)=\mathrm{Re\,Tr}[I-U(\mathcal{C})], \tag{2.7}$$

where $U(\mathcal{C})$ is the ordered product of the link variables along loop $\mathcal{C}$ contained in the set $\mathcal{S}_0$(plaquette) or $\mathcal{S}_1$(rectangular). $\mathcal{S}_0$ and $\mathcal{S}_1$ consist of all loops of the given shape that can be drawn on the cylindrical lattice with volume $L^3\times L$. The loops involve only the "dynamical links" in the sense specified above, and spatial links on the boundaries at $x_0=0$ and $x_0=L$. In particular, rectangles protruding from the boundary of the cylinder are not included.

One has to choose appropriate boundary weights to achieve 1-loop level $O(a)$ improvement for observables involving a derivative with respect to the boundary. Among various choices to achieve this, ours is given as follows:

$$W_0(\mathcal{C},g_0^2)=\begin{cases} c_{\rm s}(g_0^2) & \text{for } \mathcal{C}\in P_{\rm s}\text{: set of plaquettes that lie on one of the boundaries,}\\ c_0c_{\rm t}^P(g_0^2) & \text{for } \mathcal{C}\in P_{\rm t}\text{: set of plaquettes that just touch one of the boundaries,}\\ c_0 & \text{for } \mathcal{C}\in P_{\rm other}\text{: otherwise,}\end{cases} \tag{2.8}$$

$$W_1(\mathcal{C},g_0^2)=\begin{cases} 0 & \text{for } \mathcal{C}\in R_{\rm s}\text{: set of rectangles that lie completely on one of the boundaries,}\\ c_1c_{\rm t}^R(g_0^2) & \text{for } \mathcal{C}\in R_{\rm t}^2\text{: set of rectangles that have exactly two links on a boundary,}\\ c_1 & \text{for } \mathcal{C}\in R_{\rm other}\text{: otherwise,}\end{cases} \tag{2.9}$$

with

$$c_0c_{\rm t}^P(g_0^2)=c_0[1+c_{\rm t}^{P(1)}g_0^2+O(g_0^4)], \tag{2.10}$$

$$c_1c_{\rm t}^R(g_0^2)=c_1[3/2+c_{\rm t}^{R(1)}g_0^2+O(g_0^4)], \tag{2.11}$$

where the coefficients c_0 and c_1 of the improved gauge action are normalized such that $c_0+8c_1=1$. We call $c_{\rm t}^P(g_0^2)$ and $c_{\rm t}^R(g_0^2)$ $O(a)$ boundary improvement coefficients. So far, the 1-loop coefficients $c_{\rm t}^{P(1)}$ and $c_{\rm t}^{R(1)}$ are independent of each other. The weight factors $W_i(\mathcal{C},g_0^2)$, which include the loop corrections, become choice B of [11] in the weak coupling limit. Choice B achieves the tree-level $O(a)$ improvement and, at the same time, the lattice background field V in Eq. (2.3) satisfies the equation of motion obtained by the variation of dynamical links.

Incidentally, we discuss the $O(a)$ boundary counterterm from a different point of view. Here, it is assumed that the

plaquette loops and rectangle loops which lie completely on the cylinder $L^3\times L$ are included in the action, and that each boundary consists of one time slice only. As explained in [1], at order a in the pure gauge theory, there are two possible boundary counterterms, $a^4\,\mathrm{Tr}\{F_{0k}F_{0k}\}$ and $a^4\,\mathrm{Tr}\{F_{kl}F_{kl}\}$, each of which is summed over the $x_0=0$ or $x_0=L$ hyperplane. Since the latter boundary term vanishes in the case of an Abelian constant boundary field, in the following, we consider only the former. In this case, we have three candidates for $O(a)$ boundary counterterms that respect lattice symmetries,

(1) the spatial sum of timelike plaquette loops that just touch one of the boundaries,
(2) the spatial sum of rectangle loops that have exactly two links on a boundary,
(3) the spatial sum of rectangle loops that have exactly one link on a boundary,

to satisfy one condition, the $O(a)$ improvement condition. Therefore, for simplicity, we can take a trivial weight for the term 3, and we still have one degree of freedom for the choice of the boundary terms. At the tree level, however, the background field given in Eq. (2.3) must satisfy the equation of motion,[1] so that one has to take $c_t^P=1$ and $c_t^R=3/2$ (choice B). Since no such extra constraint exists for the 1-loop boundary terms, we can freely set the relation between $c_{\mathrm{t}}^{P(1)}$ and $c_{\mathrm{t}}^{R(1)}$, which will be given in the next section.

III. SF COUPLING AND $O(a)$ BOUNDARY IMPROVEMENT COEFFICIENTS

The SF with the improved gauge action is given by

$$\mathcal{Z}=e^{-\Gamma}=\int D[U]e^{-S[U]}, \tag{3.1}$$

where $S[U]=S_{\mathrm{imp}}[U]$. We require the same boundary condition Eq. (2.2) for the link variables as in the case of the Wilson plaquette action. In perturbative calculations, there are two main concerns to note: one is whether the background field given by Eq. (2.3) corresponds to the absolute minimum of the action, and the other is the gauge fixing. For the latter, we used the covariant gauge fixing procedure outlined in [1]. The former statement is positively proved in [1] for the Wilson plaquette action. Unfortunately, the statement has not been proved yet in the case of improved gauge actions, since the proof in [1] is not applicable to these cases. In [9], however, it was numerically checked that the background field given in Eq. (2.3) corresponds to the minimum for a large class of improved actions; hence we assume this in our perturbative calculations.

In a neighborhood of the background field V, any link variables U can be parametrized by

$$U(x,\mu)=\exp\{g_0 a q_\mu(x)\}V(x,\mu), \tag{3.2}$$

where q_μ are quantum fields. The SF coupling is defined through the free energy Γ in Eq. (3.1):

$$\overline{g}^2_{\mathrm{SF}}(L)=\left.\frac{\Gamma'_0}{\Gamma'}\right|_{\eta=\nu=0}, \tag{3.3}$$

where Γ' is the derivative with respect to η. Γ'_0 is a normalization constant

$$\begin{aligned}\Gamma'_0&=\left.\frac{\partial}{\partial\eta}g_0^2S[V]\right|_{g_0^2=0}\\&=\frac{\partial}{\partial\eta}[c_0g_0^2S_{\mathrm{plaq}}[V]|_{g_0^2=0}+c_1g_0^2S_{\mathrm{rect}}[V]|_{g_0^2=0}],\end{aligned} \tag{3.4}$$

with

$$\begin{aligned}\left.\frac{\partial}{\partial\eta}g_0^2S_{\mathrm{plaq}}[V]\right|_{g_0^2=0}&=\frac{\partial}{\partial\eta}\left[c_t^P(g_0^2)\sum_{P_{\mathrm{t}}}2\mathcal{L}(C)\right.\\&\qquad\left.+\sum_{P_{\mathrm{other}}}2\mathcal{L}(C)\right]\Big|_{g_0^2=0}\Big|_{U=V}\\&=12\left(\frac{L}{a}\right)^2(\sin 2\gamma+\sin\gamma)\\&=\Gamma'^{\,\mathrm{cont}}_0+O(a^4),\end{aligned} \tag{3.5}$$

$$\begin{aligned}\left.\frac{\partial}{\partial\eta}g_0^2S_{\mathrm{rect}}[V]\right|_{g_0^2=0}&=\frac{\partial}{\partial\eta}\left[c_t^R(g_0^2)\sum_{R_{\mathrm{t}}^2}2\mathcal{L}(C)\right.\\&\qquad\left.+\sum_{R_{\mathrm{other}}}2\mathcal{L}(C)\right]\Big|_{g_0^2=0}\Big|_{U=V}\\&=12\cdot4\left(\frac{L}{a}\right)^2(\sin 4\gamma+\sin 2\gamma)\\&=8\Gamma'^{\,\mathrm{cont}}_0+O(a^4),\end{aligned} \tag{3.6}$$

where γ is given in the Appendix and $\Gamma'^{\,\mathrm{cont}}_0=12\pi$ (if $\eta=0$), normalization in the continuum theory.

Let us discuss the perturbative expansion of the SF coupling. Making use of the facts that

$$\sum_{P_{\mathrm{t}}}2\mathcal{L}(C)\Big|_{U=V}=\frac{2a}{L}g_0^2S_{\mathrm{plaq}}[V]\Big|_{g_0^2=0}, \tag{3.7}$$

$$\sum_{R_{\mathrm{t}}^2}2\mathcal{L}(C)\Big|_{U=V}=\frac{a}{L}g_0^2S_{\mathrm{rect}}[V]\Big|_{g_0^2=0}, \tag{3.8}$$

one finds that

[1]The equation of motion for the plaquette action is trivially satisfied.

$$g_0^2 S[V] = \Gamma_0 + g_0^2 \frac{2a}{L}\Big[c_0 c_t^{P(1)}(g_0^2 S_{\rm plaq}[V]|_{g_0^2=0}) + \frac{1}{2} c_1 c_t^{R(1)}(g_0^2 S_{\rm rect}[V]|_{g_0^2=0})\Big] + O(g_0^4). \tag{3.9}$$

Then perturbative expansion of $\overline{g^2_{\rm SF}}(L)$ is given by

$$\overline{g^2_{\rm SF}}(L) = g_0^2 + m_1^{(1)}(L/a) g_0^4 + O(g_0^6), \tag{3.10}$$

with

$$m_1^{(1)}(L/a) = -\frac{1}{\Gamma_0'}\frac{2a}{L}\frac{\partial}{\partial\eta}\Big[c_0 c_t^{P(1)}(g_0^2 S_{\rm plaq}[V]|_{g_0^2=0}) + \frac{1}{2} c_1 c_t^{R(1)}(g_0^2 S_{\rm rect}[V]|_{g_0^2=0})\Big] + m_1^{(0)}(L/a), \tag{3.11}$$

where $m_1^{(0)}(L/a)$ is the 1-loop correction to the SF coupling calculated with the tree-level $O(a)$ boundary coefficients, and the details of the calculation will be given in the next section. Here, if we require that $c_t^{P(1)}$ and $c_t^{R(1)}$ satisfy (this is possible by using the last degree of freedom as mentioned at the end of the previous section)

$$c_t^{R(1)} = 2 c_t^{P(1)}, \tag{3.12}$$

and introduce $c_t^{(1)}$

$$c_t^{(1)} = c_0 c_t^{P(1)} + 4 c_1 c_t^{R(1)} = c_t^{P(1)}, \tag{3.13}$$

then we find $m_1^{(1)}(L/a)$ in a very simple form:

$$m_1^{(1)}(L/a) = -\frac{2a}{L} c_t^{(1)} + m_1^{(0)}(L/a). \tag{3.14}$$

If we do not require Eq. (3.12), but use another choice, then we find

$$m_1^{(1)}(L/a) = -\frac{2a}{L}[c_t^{(1)} + O(a^4)] + m_1^{(0)}(L/a), \tag{3.15}$$

where $m_1^{(0)}(L/a)$ is the same as in Eq. (3.14) and there is an $O(a^4)$ contribution coming from boundary terms at the tree level. The differences between the choice Eq. (3.12) and other choices of $c_t^{P(1)}, c_t^{R(1)}$ reflect just the $O(a^5)$ contribution in $m_1^{(1)}(L/a)$. Therefore, the differences between their scaling violations are tiny at 1-loop order. In the following, we take the choice Eq. (3.12).

The value of the 1-loop coefficient $c_t^{(1)}$ is determined by the condition that the dominant part of the scaling violation of $m_1^{(1)}(L/a)$ should be proportional to $(a/L)^2$, and then $c_t^{P(1)}$ and $c_t^{R(1)}$ are uniquely given by Eq. (3.12) and Eq. (3.13).

IV. CALCULATION OF THE ONE-LOOP COEFFICIENT

In the following, we choose lattice units (i.e., $a=1$). According to the unpublished note [12], we have used I^a ($a=1,2,\ldots,8$) as the basis of the Lie algebra of SU(3) in the presence of the background field. Their explicit form can be found in [13]. Decomposing in the basis I^a,

$$q_\mu(x) = \sum_a \tilde{q}_\mu^a(x) I^a, \tag{4.1}$$

the quantum fields q_μ are Fourier transformed with respect to spatial momenta as

$$\tilde{q}_0^a(x) = \frac{1}{L^3}\sum_{\mathbf{p}} e^{i\mathbf{p}\mathbf{x}} \tilde{q}_0^a(\mathbf{p}, x_0), \tag{4.2}$$

$$\tilde{q}_k^a(x) = \frac{1}{L^3}\sum_{\mathbf{p}} e^{i\mathbf{p}\mathbf{x}} e^{i[p_k + \phi_a(x_0)]/2} \tilde{q}_k^a(\mathbf{p}, x_0), \tag{4.3}$$

where the phase $\phi_a(x_0)$ is given in the Appendix. In terms of $\tilde{q}_\mu^a(x)$, the quadratic part of the improved gauge action Eq. (2.6) takes the form

$$S_{\rm imp}^{(0)} = \frac{1}{L^3}\sum_{\mathbf{p}} \sum_{x_0, y_0=0}^{L-1} \sum_a \bar{\tilde{q}}_\mu^a(-\mathbf{p}, x_0) K_{\mu\nu}^a(\mathbf{p}; x_0, y_0) \times \tilde{q}_\nu^a(\mathbf{p}, y_0), \tag{4.4}$$

with the condition

$$\tilde{q}_k^a(\mathbf{p}, x_0)|_{x_0=0} = 0 \quad \text{for } k=1,2,3. \tag{4.5}$$

The explicit form of the inverse propagator $K_{\mu\nu}^a$ is given in [11], and also in the Appendix.

As in the case of the Wilson plaquette action [1], the 1-loop correction $m_1^{(0)}(L)$ in the case of an improved action is given by

$$m_1^{(0)}(L) = -\frac{1}{\Gamma_0'}\frac{\partial}{\partial\eta}\Big[\frac{1}{2}\ln \mathrm{Det} K - \ln \mathrm{Det}\,\Delta_0\Big]\Big|_{\eta=\nu=0}, \tag{4.6}$$

where the determinant for the quantum field sector (the first term in the right hand side of the equation) is taken with respect to the spatial momentum $\mathbf{p}$, the time x_0, the Lie algebra sector a, and the Lorentz index μ. The second term in the right hand of Eq. (4.6) represents a contribution from the ghost sector. The differential operator for the ghost sector is given by

$$\Delta_0 = -d^* d, \tag{4.7}$$

where d is a linear operator and defined as $(dw)_\mu(x) = D_\mu w(x)$ for proper $w(x)$, the generators of the gauge transformation satisfying nontrivial boundary conditions [1]. d^* is defined as the negative adjoint of d. Here we will exclusively consider the quantum field sector, since the con-

TABLE I. One-loop coefficient $m_1^{(0)}(L)$ for improved actions.

L	Iwasaki action	LW action	DBW2 action
6	0.0865021015584032	0.3843092560841445	−0.2542597063902088
7	0.1026697312426737	0.4061279685078025	−0.2517151449619943
8	0.1171638577366678	0.4249279311929165	−0.2462340808659547
9	0.1303628849788211	0.4414718008748639	−0.2394316692834335
10	0.1424404981803593	0.4562496675217995	−0.2322864496797361
11	0.1535565273026473	0.4696045216347286	−0.2251762317750280
12	0.1638489264935022	0.4817875167578513	−0.2182314272034601
13	0.1734301653189940	0.4929883879248706	−0.2114993870451222
14	0.1823916642888328	0.5033540747374835	−0.2049961094379959
15	0.1908085280119190	0.5130007428050310	−0.1987234947986162
16	0.1987431354745856	0.5220218429952182	−0.1926766886112917
17	0.2062478088988484	0.5304936855855431	−0.1868475754585161
18	0.2133668331494581	0.5384793988419066	−0.1812265016307355
19	0.2201380038925787	0.5460318047790646	−0.1758031806343642
20	0.2265938267004754	0.5531955499144914	−0.1705672082184823
21	0.2327624550322364	0.5600087116401930	−0.1655083693982648
22	0.2386684311658198	0.5665040280450621	−0.1606168213494539
23	0.2443332770354413	0.5727098525006191	−0.1558831969805698
24	0.2497759696349747	0.5786509038428871	−0.1512986565129531
25	0.2550133267993803	0.5843488625662739	−0.1468549050440217
26	0.2600603227656853	0.5898228494962823	−0.1425441882890768
27	0.2649303482326239	0.5950898137064368	−0.1383592748238773
28	0.2696354261875951	0.6001648495876492	−0.1342934304660328
29	0.2741863922040979	0.6050614580595203	−0.1303403885609065
30	0.2785930459882241	0.6097917633368525	−0.1264943186395051
31	0.2828642794964034	0.6143666940320125	−0.1227497950252100
32	0.2870081858351735	0.6187961354134090	−0.1191017663623826
33	0.2910321522986861	0.6230890581649763	−0.1155455266354859
34	0.2949429402366960	0.6272536278701680	−0.1120766879801252
35	0.2987467539279429	0.6312972985837565	−0.1086911554135926
36	0.3024493002264770	0.6352268931891717	−0.1053851035018207
37	0.3060558404258739	0.6390486727199947	−0.1021549549113093
38	0.3095712355291510	0.6427683964162490	−0.0989973607544213
39	0.3129999859059953	0.6463913739632261	−0.0959091826148500
40	0.3163462661525911	0.6499225111032890	−0.0928874761305482
41	0.3196139558344332	0.6533663496047807	−0.0899294760096131
42	0.3228066666825220	0.6567271024057376	−0.0870325823576189
43	0.3259277667231945	0.6600086846150990	−0.0841943482007244
44	0.3289804017476282	0.6632147409439818	−0.0814124680962679
45	0.3319675144656546	0.6663486700493243	−0.0786847677306482
46	0.3348918616375112	0.6694136461978401	−0.0760091944125418
47	0.3377560294345988	0.6724126385966856	−0.0733838083775785
48	0.3405624472446620	0.6753484286860957	−0.0708067748282852

tribution from the ghost sector to the 1-loop correction is same as in the case of the Wilson plaquette action. Our boundary condition for the temporal component q_0 is different from that in [1], so that the ''non-uniform'' contribution in the gauge fixing term remains in the inverse propagator K (see the Appendix).

We evaluated the 1-loop correction $m_1^{(0)}(L)$ numerically for the Iwasaki action ($c_1=-0.331$, $c_2=c_3=0$) [14], the Lüscher-Weisz (LW) action ($c_1=-1/12$, $c_2=c_3=0$) [15], and the DBW2 action ($c_1=-1.40686$, $c_2=c_3=0$) [16] in the range $L=6,\ldots,48$. The results are shown in Table I. The computations have been performed by using FORTRAN with extended precision. As a check of our calculation, we confirmed the independence of the gauge fixing parameter and the expected symmetries before reducing the amount of calculation [17]. We also checked that our code at $c_1=0$ reproduces the known results for the Wilson plaquette action [18]. Furthermore, two codes written independently by the

TABLE II. The coefficients of asymptotic expansion A_0, A_1 for various gauge actions. The values for the plaquette action are taken from [8,18]. Since the error of $A_0^{\rm exp}$ for the DBW2 action is not given (see footnote 2), the quoted digits are of little significance.

	Plaquette action	Iwasaki action	LW action	DBW2 action
A_0	0.36828215(13)	−0.2049015(4)	0.136150567(6)	−0.62776(8)
$A_0^{\rm exp}$		−0.1999(24)	0.13621(26)	−0.62
A_1	−0.17800(10)	0.30360(26)	−0.005940(2)	0.896(45)

two authors produced identical results up to about 30 digits in the range $L=6,\ldots,32$. Beyond this range, we used the faster code only.

V. ANALYSIS AND RESULTS

In this section we extract the order $1/L$ term from the 1-loop correction $m_1^{(0)}(L)$ to determine the $O(a)$ boundary improvement coefficient $c_{\rm t}^{(1)}$. According to Symanzik's analysis of the cutoff dependence of Feynman diagrams on the lattice, one expects that the 1-loop coefficient has the asymptotic expansion

$$m_1^{(0)}(L) \overset{L\to\infty}{\sim} \sum_{n=0}^{\infty} (A_n + B_n \ln L)/L^n. \tag{5.1}$$

Using the blocking method of [19], we extracted the first few coefficients A_0, B_0, A_1, B_1, and estimated their errors.

Some of these coefficients are known or related to other quantities. For example, the A_0's of two different actions are related to the ratio of the Λ parameters of the two actions. If the ultraviolet divergence in the SF is removed by the standard renormalization of the coupling constant, $B_0=2b_0$, where $b_0=11/(4\pi)^2$ is the 1-loop coefficient of the β function in pure SU(3) gauge theory. If the tree-level $O(a)$ improvement is implemented, $B_1=0$ must hold. Our main result comes from A_1: Eq. (3.14) gives $c_{\rm t}^{(1)}=A_1/2$.

We first verified that our extraction of B_0 and B_1 is consistent with the above expectations. We confirmed that $B_0=2b_0$ up to seven digits (Iwasaki), nine digits (LW), or four digits (DBW2), while $B_1<10^{-4}$ (Iwasaki), $<10^{-7}$ (LW), or $<10^{-2}$ (DBW2). Since our data give the expected values of B_0 and B_1, we fix $B_0=2b_0$ and $B_1=0$ by hand in the blocking procedure to extract A_0 and A_1, whose results for each action are shown in Table II where we have added the result of the plaquette action [8,18] for later reference.

As a further check, we extract the A_0's from the ratio of the Λ parameters between two schemes X and Y, which is given by

$$\frac{\Lambda_X}{\Lambda_Y} = e^{-c/2b_0}, \tag{5.2}$$

where

$$\overline{g}_Y^2(\mu) = \overline{g}_X^2(\mu) + c\overline{g}_X^4(\mu) + \cdots. \tag{5.3}$$

The purely numerical number c here is given by

$$c = A_0^X - A_0^Y, \tag{5.4}$$

where A_0^X or A_0^Y is the expected A_0 of the scheme X or Y, respectively. We then find

$$A_0^{\rm imp} = A_0^{\rm plaq} - 2b_0 \ln\left[\frac{\Lambda_{\rm imp}}{\Lambda_{\rm plaq}}\right]. \tag{5.5}$$

Using $A_0^{\rm plaq}=0.36828215(13)$ [8,18] and the ratio of the Λ parameters[2]

$$\frac{\Lambda_{\rm imp}}{\Lambda_{\rm plaq}} = \begin{cases} 59.05\pm 1.0 & \text{for the Iwasaki action [21],} \\ 5.29\pm 0.01 & \text{for the LW action [22],} \\ 13\times 10^2 & \text{for the DBW2 action [23],} \end{cases} \tag{5.6}$$

we obtain the values of $A_0^{\rm imp}$ for each action that is shown in Table II ($A_0^{\rm exp}$). We observed consistency in A_0 between previous known results and our calculations.

With this confidence in our computation, we obtain the main result of our paper, the one-loop $O(a)$ boundary improvement coefficient Eq. (3.14), which is given by

$$c_{\rm t}^{(1)} = c_{\rm t}^{P(1)} = A_1/2, \tag{5.7}$$

where A_1 is also found in Table II.

Finally, using our results for A_0 in Table II, we can estimate the ratio of the Λ parameters between the improved action and the plaquette action more accurately:

$$\frac{\Lambda_{\rm imp}}{\Lambda_{\rm plaq}} = \frac{\Lambda_{\rm imp}/\Lambda_{\rm SF}}{\Lambda_{\rm plaq}/\Lambda_{\rm SF}} = \exp\left\{\frac{1}{2b_0}[A_0^{\rm plaq} - A_0]\right\}$$
$$= \begin{cases} 61.2064(3) & \text{for the Iwasaki action,} \\ 5.292104(5) & \text{for the LW action,} \\ 1273.4(8) & \text{for the DBW2 action.} \end{cases} \tag{5.8}$$

VI. CONCLUSIONS AND DISCUSSION

Combining our result for $c_{\rm t}^{(1)}$ for the improved gauge actions and the previous result for $c_{\rm t}^{(1)}$ for the clover quark action [7], we obtain

[2]We take the value for the DBW2 action from a private note [23], where the error of the value was not given; therefore the quoted digits are of little significance.

TABLE III. The deviations for various gauge actions.

	Plaquette action		Iwasaki action		LW action		DBW2 action	
L	$\delta_1^{(0)}$	$\delta_1^{(1)}$	$\delta_1^{(0)}$	$\delta_1^{(1)}$	$\delta_1^{(0)}$	$\delta_1^{(1)}$	$\delta_1^{(0)}$	$\delta_1^{(1)}$
6	0.01089	−0.00394	−0.01922	0.00608	0.000911	0.000417	−0.061	0.014
7	0.01004	−0.00268	−0.01684	0.00484	0.000659	0.000236	−0.050	0.014
8	0.00918	−0.00194	−0.01499	0.00399	0.000527	0.000156	−0.043	0.013
9	0.00841	−0.00148	−0.01356	0.00330	0.000441	0.000111	−0.038	0.011
10	0.00773	−0.00117	−0.01241	0.00277	0.000379	0.000082	−0.035	0.010
11	0.00714	−0.00095	−0.01146	0.00235	0.000333	0.000063	−0.032	0.009
12	0.00663	−0.00079	−0.01064	0.00201	0.000296	0.000049	−0.030	0.008
13	0.00618	−0.00066	−0.00994	0.00174	0.000268	0.000039	−0.028	0.007
14	0.00579	−0.00057	−0.00932	0.00152	0.000244	0.000032	−0.026	0.006
15	0.00544	−0.00049	−0.00878	0.00134	0.000224	0.000026	−0.024	0.006
16	0.00513	−0.00043	−0.00830	0.00119	0.000207	0.000022	−0.023	0.005
17	0.00486	−0.00038	−0.00787	0.00106	0.000193	0.000018	−0.022	0.005
18	0.00461	−0.00034	−0.00748	0.00095	0.000181	0.000016	−0.021	0.004
19	0.00438	−0.00030	−0.00713	0.00086	0.000170	0.000013	−0.020	0.004
20	0.00418	−0.00027	−0.00681	0.00078	0.000160	0.000012	−0.019	0.004
21	0.00399	−0.00025	−0.00652	0.00071	0.000151	0.000010	−0.018	0.003
22	0.00382	−0.00022	−0.00625	0.00065	0.000144	0.000009	−0.017	0.003
23	0.00367	−0.00020	−0.00601	0.00059	0.000137	0.000008	−0.017	0.003
24	0.00352	−0.00019	−0.00578	0.00054	0.000131	0.000007	−0.016	0.003

$$c_t^{P(1)} = c_t^{R(1)}/2 = A_1/2 + n_f c_t^{F(1)} \tag{6.1}$$

for n_f-flavor QCD, where $c_t^{F(1)} = 0.0191410(1)$.

As a final remark, let us discuss the lattice artifact of the step scaling function (SSF) [20] for various gauge actions. The SSF $\sigma(s,u)$ describes the evolution of a renormalized coupling under a finite rescaling factor s (say $s=2$)

$$\sigma(s,u) = \bar{g}^2(sL)\big|_{u=\bar{g}^2(L)}, \tag{6.2}$$

and it has the perturbative expansion

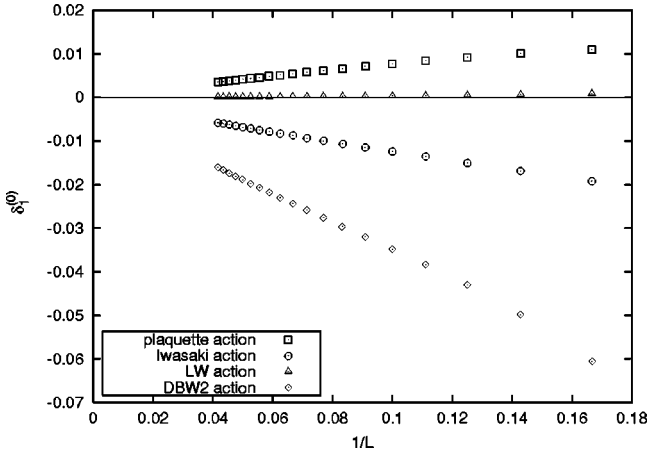

FIG. 1. The relative deviations of the lattice SSF from the continuum one at 1 loop for various gauge actions with the tree-level $O(a)$ improved boundary term. One can see that the $\delta_1^{(0)}$ for various gauge actions vanish roughly linearly in $1/L$.

$$\sigma(s,u) = u + 2b_0 \ln(s) u^2 + O(u^3). \tag{6.3}$$

This SSF $\sigma(s,u)$ in the continuum theory is obtained from the continuum limit of the lattice SSF $\Sigma(s,u,1/L)$

$$\sigma(s,u) = \lim_{1/L \to 0} \Sigma(s,u,1/L). \tag{6.4}$$

Therefore we can estimate the lattice artifact of the SSF in our perturbative calculation. We define the relative deviation $\delta(s,u,1/L)$ and expand it as

$$\delta(2,u,1/L) = \frac{\Sigma(2,u,1/L) - \sigma(2,u)}{\sigma(2,u)} = \delta_1^{(k)}(2,1/L)u + O(u^2), \tag{6.5}$$

where we have set $s=2$, and $\delta_1^{(k)}(2,1/L)$ is the 1-loop coefficient. Here k denotes the degree of improvement for the boundary coefficient: the tree (1-loop) value is used for $k=0$ $(k=1)$.

The manifest form of $\delta_1^{(k)}(2,1/L)$ is given by

$$\delta_1^{(k)}(2,1/L) = m_1^{(k)}(2L) - m_1^{(k)}(L) - 2b_0 \ln(2), \tag{6.6}$$

and the results, including data for the plaquette action [8,18] for comparison,[3] are given in Table III for each gauge action. Figure 1 (Fig. 2) shows that the 1-loop deviations with the tree-level (1-loop level) $O(a)$ improved boundary coefficient vanish roughly linearly (quadratically) in $1/L$ as expected. As

[3]We have added data for the plaquette action in the range $L=17,\ldots,24$.

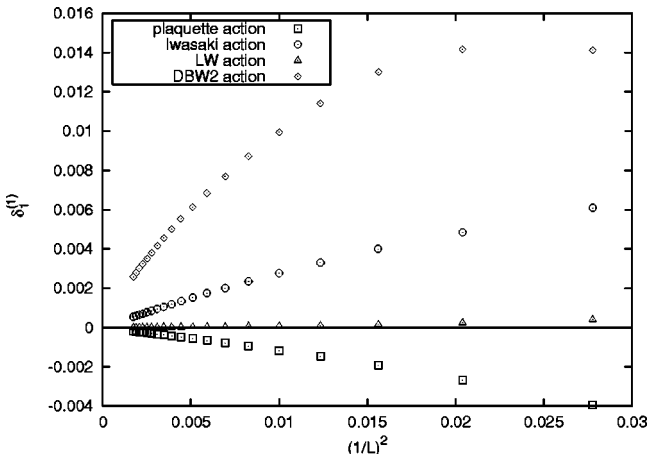

FIG. 2. The same quantities as in Fig. 1, but with the 1-loop level $O(a)$ improved boundary term. One can see that the $\delta_1^{(1)}$ for various gauge actions vanish roughly quadratically in $1/L$.

is evident from Fig. 1 and Fig. 2, at the 1-loop level, the lattice artifact for the renormalization group improved action (Iwasaki or DBW2) is comparable to or larger than that for the plaquette action, while the LW action is the least affected by the lattice cutoff. However, one cannot conclude that the LW action is the best choice for numerical simulations, where lattice artifacts of higher orders in u or a may not be negligible.

ACKNOWLEDGMENT

S.T. would like to thank Dr. Saito for informative correspondence.

APPENDIX: INVERSE PROPAGATOR

Here, we give the explicit form of the inverse propagator. We choose lattice units (i.e., $a=1$) and set $T=L$:

$$K=c_0K^{(0)}+c_1K^{(1)}+\lambda_0K^{(\mathrm{gf})}. \tag{A1}$$

1. Plaquette

$$K_{00}^{(0)a}(\mathbf{p};x_0,y_0)=R^a\delta_{x_0,y_0}\mathbf{s}^a(\mathbf{p},x_0)\cdot\mathbf{s}^a(\mathbf{p},x_0+1), \tag{A2}$$

$$K_{k0}^{(0)a}(\mathbf{p};x_0,y_0)=iR^a[\,\delta_{x_0,y_0}s_k^a(\mathbf{p},x_0+1) - \delta_{x_0-1,y_0}s_k^a(\mathbf{p},y_0)], \tag{A3}$$

$$K_{0k}^{(0)a}(\mathbf{p};x_0,y_0)=-K_{k0}^{(0)a}(\mathbf{p};y_0,x_0), \tag{A4}$$

$$K_{kl}^{(0)a}(\mathbf{p};x_0,y_0)=\delta_{x_0,y_0}[\,\delta_{kl}\mathbf{s}^a(\mathbf{p},x_0)^2 - s_k^a(\mathbf{p},x_0)s_l^a(\mathbf{p},x_0)]+\delta_{kl}[2C^a\delta_{x_0,y_0} - R^a(\delta_{x_0+1,y_0}+\delta_{x_0-1,y_0})]. \tag{A5}$$

2. Rectangle

$w_{dbc}=3/2$ for the choice B [11]:

$$K_{00}^{(1)a}(\mathbf{p};x_0,y_0)_{0kk}=\delta_{x_0,y_0}[1+(w_{dbc}-1)(\delta_{x_0,0}+\delta_{x_0,L-1})] \times 4R_2^a\sum_m \sin[\phi_a(x_0)+p_m] \times\sin[\phi_a(x_0+1)+p_m], \tag{A6}$$

$$K_{00}^{(1)a}(\mathbf{p};x_0,y_0)_{00k}=R_2^a\sum_m\{\delta_{x_0,y_0}[(1-\delta_{x_0,L-1})s_m^a(\mathbf{p},x_0) \times s_m^a(\mathbf{p},x_0+2)+(1-\delta_{x_0,0}) \times s_m^a(\mathbf{p},x_0-1)s_m^a(\mathbf{p},x_0+1)] + \delta_{x_0-1,y_0}s_m^a(\mathbf{p},x_0-1)s_m^a(\mathbf{p},x_0+1) + \delta_{x_0+1,y_0}s_m^a(\mathbf{p},y_0-1)s_m^a(\mathbf{p},y_0+1)\}, \tag{A7}$$

$$K_{k0}^{(1)a}(\mathbf{p};x_0,y_0)_{0kk}=iR_2^a2c_k^a(\mathbf{p},x_0)[\delta_{x_0,y_0}\{1+(w_{dbc}-1) \times\delta_{x_0,L-1}\}\sin[\phi_a(x_0+1)+p_k] - \delta_{x_0-1,y_0}\{1+(w_{dbc}-1)\delta_{x_0,1}\} \times\sin[\phi_a(y_0)+p_k]], \tag{A8}$$

$$K_{k0}^{(1)a}(\mathbf{p};x_0,y_0)_{00k}=iR_2^a\{s_k^a(\mathbf{p},x_0+2)[(1-\delta_{x_0,L-1}) \times\delta_{x_0,y_0}+\delta_{x_0+1,y_0}]-s_k^a(\mathbf{p},x_0-2) \times[(1-\delta_{x_0,1})\delta_{x_0-1,y_0}+\delta_{x_0-2,y_0}]\}, \tag{A9}$$

$$K_{0k}^{(1)a}(\mathbf{p};x_0,y_0)=-K_{k0}^{(1)a}(\mathbf{p};y_0,x_0), \tag{A10}$$

$$K_{kl}^{(1)a}(\mathbf{p};x_0,y_0)_{0kk}=\delta_{kl}c_k^a(\mathbf{p},x_0)c_k^a(\mathbf{p},y_0) \times[2C_2^a\delta_{x_0,y_0}-R_2^a(\delta_{x_0+1,y_0}+\delta_{x_0-1,y_0})] +(w_{dbc}-1)\delta_{kl}\delta_{x_0,y_0}c_k^a(\mathbf{p},x_0) \times[\delta_{x_0,1}[C_2^ac_k^a(\mathbf{p},x_0)-iS_2^as_k^a(\mathbf{p},x_0)] + \delta_{x_0,L-1}[C_2^ac_k^a(\mathbf{p},x_0) +iS_2^as_k^a(\mathbf{p},x_0)]], \tag{A11}$$

TABLE IV. C^a and S^a for SU(3).

a	C^a	S^a
1,4	$(\cos 2\gamma+\cos\gamma)/2$	$-i(\sin 2\gamma+\sin\gamma)/2$
3,6	$\cos\gamma$	0
8	$(2\cos 2\gamma+\cos\gamma)/3$	0

TABLE V. $\phi_a(x_0)$ and R^a for SU(3).

a	$\phi_a(x_0)$	R^a
1	$-3\gamma x_0+(1/L)(\eta[3/2-\nu]-\pi/3)$	$\cos(\gamma/2)$
4	$-3\gamma x_0+(1/L)(\eta[3/2+\nu]-2\pi/3)$	$\cos(\gamma/2)$
3	0	$\cos\gamma$
6	$(1/L)(2\eta\nu-\pi/3)$	$\cos\gamma$
8	0	$(2\cos 2\gamma+\cos\gamma)/3$

$$K_{kl}^{(1)a}(\mathbf{p};x_0,y_0)_{\text{others}}=\delta_{x_0,y_0}\Big[\delta_{kl}\sum_m s_m^a(\mathbf{p},x_0)^2 \times[c_k^a(\mathbf{p},x_0)^2+c_m^a(\mathbf{p},x_0)^2]-s_k^a(\mathbf{p},x_0) \times s_l^a(\mathbf{p},x_0)[c_k^a(\mathbf{p},x_0)^2+c_l^a(\mathbf{p},x_0)^2]\Big] + \delta_{kl}[(2-\delta_{x_0,1}-\delta_{x_0,L-1})C_2^a\delta_{x_0,y_0} - R_2^a(\delta_{x_0+2,y_0}+\delta_{x_0-2,y_0})]. \quad \text{(A12)}$$

3. Gauge fixing term

$$K_{00}^{(\mathrm{gf})a}(\mathbf{p};x_0,y_0)=2\delta_{x_0,y_0}-\delta_{x_0+1,y_0}-\delta_{x_0-1,y_0} - \delta_{x_0,y_0}[\delta_{x_0,0}(1-\chi_a\delta_{\mathbf{p},\mathbf{0}})+\delta_{x_0,L-1}], \quad \text{(A13)}$$

$$K_{k0}^{(\mathrm{gf})a}(\mathbf{p};x_0,y_0)=-is_k^a(\mathbf{p},x_0)[\delta_{x_0,y_0}-\delta_{x_0-1,y_0}], \quad \text{(A14)}$$

$$K_{0k}^{(\mathrm{gf})a}(\mathbf{p};x_0,y_0)=-K_{k0}^{(\mathrm{gf})a}(\mathbf{p};y_0,x_0), \quad \text{(A15)}$$

TABLE VI. R_2^a, C_2^a and S_2^a for SU(3).

a	R_2^a	C_2^a	S_2^a
1,4	$\cos\gamma$	$R_2^a\cos 3\gamma$	$-iR_2^a\sin 3\gamma$
3,6	$\cos 2\gamma$	R_2^a	0
8	$(2\cos 4\gamma+\cos 2\gamma)/3$	R_2^a	0

$$K_{kl}^{(\mathrm{gf})a}(\mathbf{p};x_0,y_0)=\delta_{x_0,y_0}s_k^a(\mathbf{p},x_0)s_l^a(\mathbf{p},x_0). \quad \text{(A16)}$$

4. Coefficients

$$s_k^a(\mathbf{p},x_0)=2\sin\{[p_k+\phi_a(x_0)]/2\}, \quad \text{(A17)}$$

$$c_k^a(\mathbf{p},x_0)=2\cos\{[p_k+\phi_a(x_0)]/2\}, \quad \text{(A18)}$$

$$\phi_a(x_0)=-\phi_{\bar{a}}(x_0), \quad \text{(A19)}$$

$$C^a=C^{\bar{a}},\quad S^a=-S^{\bar{a}},\quad R^a=R^{\bar{a}}, \quad \text{(A20)}$$

$$C_2^a=C_2^{\bar{a}},\quad S_2^a=-S_2^{\bar{a}},\quad R_2^a=R_2^{\bar{a}}, \quad \text{(A21)}$$

$$\chi_a=\chi_{\bar{a}}=(0,0,1,0,0,0,0,1), \quad \text{(A22)}$$

$$\gamma=\frac{1}{L^2}\left(\eta+\frac{\pi}{3}\right), \quad \text{(A23)}$$

where $\bar{1}=2$, $\bar{4}=5$, $\bar{6}=7$, and vice versa. For the diagonal part, $\bar{3}=3$, $\bar{8}=8$.

5. Lists of coefficients

The coefficients are given in Tables IV–VI.

[1] M. Lüscher, R. Narayanan, P. Weisz, and U. Wolff, Nucl. Phys. **B384**, 168 (1992).
[2] ALPHA Collaboration, A. Bode *et al.*, Phys. Lett. B **515**, 49 (2001).
[3] ALPHA Collaboration, M. Della Morte *et al.*, hep-lat/0209023.
[4] JLQCD Collaboration, S. Aoki *et al.*, Nucl. Phys. B (Proc. Suppl.) **106**, 1079 (2002).
[5] JLQCD Collaboration, S. Aoki *et al.*, Nucl. Phys. B (Proc. Suppl.) **106**, 263 (2002).
[6] CP-PACS Collaboration, S. Aoki *et al.*, hep-lat/0211034.
[7] S. Sint and R. Sommer, Nucl. Phys. **B465**, 71 (1996).
[8] M. Lüscher, R. Sommer, P. Weisz, and U. Wolff, Nucl. Phys. **B413**, 481 (1994).
[9] T. Klassen, Nucl. Phys. **B509**, 391 (1998).
[10] M. Lüscher and P. Weisz, Nucl. Phys. **B240**, 349 (1984).
[11] S. Aoki, R. Frezzotti, and P. Weisz, Nucl. Phys. **B540**, 501 (1999); and (unpublished).
[12] P. Weisz (unpublished).
[13] S. Kurth, Ph.D. thesis, Humboldt University, hep-lat/0211011.
[14] Y. Iwasaki, Nucl. Phys. **B258**, 141 (1985); University of Tsukuba Report No. UTHEP-118, 1983.
[15] M. Lüscher and P. Weisz, Commun. Math. Phys. **97**, 59 (1985); **98**, 433(E) (1985); Phys. Lett. **158B**, 250 (1985).
[16] T. Takaishi, Phys. Rev. D **54**, 1050 (1996); P. de Forcrand *et al.*, Nucl. Phys. **B577**, 263 (2000).
[17] R. Narayanan and U. Wolff, Nucl. Phys. **B444**, 425 (1995).
[18] A. Bode, U. Wolff, and P. Weisz, Nucl. Phys. **B540**, 491 (1999).
[19] M. Lüscher and P. Weisz, Nucl. Phys. **B266**, 309 (1986).
[20] M. Lüscher, P. Weisz, and U. Wolff, Nucl. Phys. **B359**, 221 (1991).
[21] Y. Iwasaki and T. Yoshie, Phys. Lett. **143B**, 449 (1984).
[22] Y. Iwasaki and S. Sakai, Nucl. Phys. **B248**, 441 (1984).
[23] S. Sakai, T. Saito, and A. Nakamura, Nucl. Phys. **B584**, 528 (2000); T. Saito (private communication).